European Journal of Chemistry

Check for updates

View Journal Online
View Article Online

A hydroxypropiophenone-based fluorescent probe for the selective determination of Al(III) ions in aqueous ethanol

Chandni Singh [1], Divya Pratap Singh [2,*], Sunil Kumar Singh [1,*], Romi Dwivedi [3], Ashish Kumar Singh [1,*] and Vinod Prasad Singh [3]

[1] *Department of Chemistry, Guru Ghasidas Vishwavidyalaya, Bilaspur-495009, India*
[2] *Department of Chemistry, Rajkiya Engineering College, Azamgarh-276201, India*
[3] *Department of Chemistry, Institute of Science, Banaras Hindu University, Varanasi-221005, India*

* *Corresponding author at: Department of Chemistry, Rajkiya Engineering College, Azamgarh-276201, India.*
e-mail: dpsingh_011@yahoo.co.in (D.P. Singh), singh.skumar@gmail.com (S.K. Singh), ashish.bhuchem@gmail.com (A.K. Singh).

RESEARCH ARTICLE

10.5155/eurjchem.14.1.99-108.2360

Received: 20 November 2022
Received in revised form: 03 January 2023
Accepted: 12 January 2023
Published online: 31 March 2023
Printed: 31 March 2023

KEYWORDS

Dihydrazone
UV-vis study
Chemical sensor
Fluorescence study
Density functional theory
Chelation-enhanced fluorescence

ABSTRACT

In this work, we have synthesized a novel dihydrazone-based fluorescent probe *N'*[1],*N'*[2]-*bis*{1-(2-hydroxyphenyl)propylidene}oxalohydrazide (H_2hpoh)for Al^{3+} ions by a simple condensation reaction. The prepared organic probe has been characterized by different physicochemical and spectroscopic techniques. The single-crystal structure of the receptor has also been reported. Crystal data for $C_{20}H_{22}N_4O_4$: monoclinic, space group $P2_1/c$ (no. 14), a = 6.0747(15) Å, b = 11.621(5) Å, c = 13.453(4) Å, β = 94.61(3)°, V = 946.6(5) Å^3, Z = 2, T = 293(2) K, μ(MoKα) = 0.096 mm^{-1}, *Dcalc* = 1.342 g/cm^3, 4046 reflections measured (6.076° ≤ 2Θ ≤ 58.05°), 2149 unique (R_{int} = 0.0876, R_{sigma} = 0.2223) which were used in all calculations. The final R_1 was 0.0972 (I > 2σ(I)) and wR_2 was 0.2316 (all data). The ethanolic aqueous solution of the probe shows enhanced fluorescence in the presence of Al^{3+} ions, whereas no appreciable change in the spectral pattern is observed in the presence of other cations, *i.e.,* Na^+, K^+, Ca^{2+}, Ba^{2+}, Mn^{2+}, Fe^{3+}, Co^{2+}, Ni^{2+}, Cu^{2+}, Zn^{2+}, Cr^{3+}, Cd^{2+} and Hg^{2+}. The binding mode of the receptor with Al^{3+} ions was studied using various spectral titration techniques such as UV-visible, fluorescence, and ^{1}H NMR. The receptor acts as a dibasic hexadentate ligand and interacts with two Al^{3+} ions with a high binding constant K_B = 8.99×10^{10} 1/M. The lowest detection limit for the Al^{3+} complex of H_2hpoh was determined to be 7.8×10^{-5} M. With the help of DFT calculations, the mechanism of fluorescence enhancement has been explained.

Cite this: *Eur. J. Chem.* **2023**, *14(1)*, 99-108 **Journal website**: www.eurjchem.com

1. Introduction

The selective identification of chemical and ionic species that are important to the environment using molecular sensors has received great attention [1-7]. Effective chemical sensors have been designed and developed using non-covalent interactions such as Vander Waal's contact, hydrogen bonding, electrostatic force, metal-ligand coordination, and hydrophobic interactions [8-10]. Govindaraju *et al.* suggested that '*Photoinduced electron transfer (PET) based sensors exhibit changes in emission intensity with little or no spectral shift, whereas internal charge transfer (ICT) sensors exhibit both intensity changes and spectral shifts*' [9]. The design of receptors for the detection of aluminum ions may be significantly influenced by the use of Schiff bases in homogeneous or heterogeneous environments. Aluminum is widely used for industrial and domestic purposes. The toxicity of aluminum towards a diversity of living beings, including humans, is also well discussed in the literature from time to time [11-14]. Aluminum in its ionic form (Al^{3+}) can react with biological species by altering or suppressing their function, leading to harmful effects. The Al^{3+}ion is neurotoxic and causes neurofibrillary, enzymatic, neurological disorders such as Parkinson's disease, Alzheimer's disease, and neurotransmitter changes in the central nervous system [15-17].

Schiff bases create an environment similar to the one present in biological systems, usually by making coordination through oxygen and nitrogen atoms [16-18]. Several significant properties of carbonic acid hydrazides, along with their applications in medicine and analytical chemistry, have led to increased interest in their complexation characteristics with transition metal ions [19,20]. Schiff bases offer several attractive structural features, such as the degree of rigidity, a conjugated π-system, and an NH unit that readily participates in hydrogen bonding and maybe a protonation-deprotonation site [21,22]. 2-Hydroxy hydrazone ligands are of interest mainly due to the existence of OH···N or O···HN type hydrogen bonds and tautomerism between the forms of phenol-imine and keto-amine[18,19].It is well recognized that the formation of metal complexes plays an important role to improve the biological activity of free hydrazones [23].

Various Al^{3+}ion sensors based on *o*-hydroxyphenyl hydrazone have already been reported by our group, as well as other scientists around the world [16-19,24-38]. The selected receptor *N'*[1], *N'*[2]-*bis*{1-(2-hydroxyphenyl) propylidene}oxalo

https://dx.doi.org/10.5155/eurjchem.14.1.99-108.2360

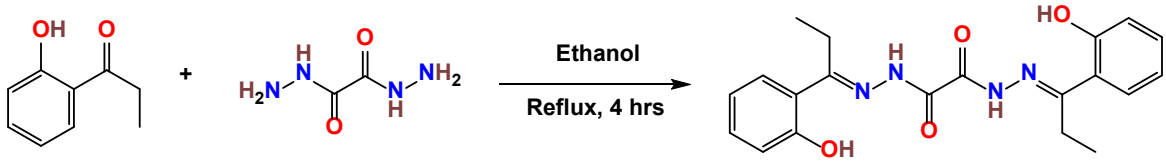

Scheme 1. Synthesis of receptor.

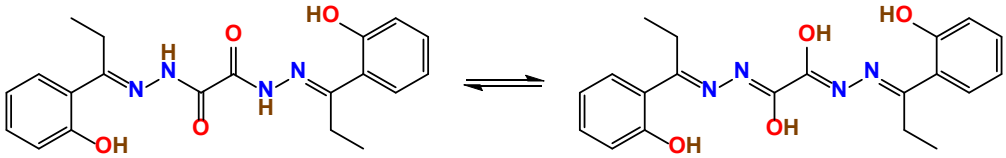

Scheme 2. Tautomerization in H_2hpoh.

hydrazide (H_2hpoh) for the present study can easily be synthesized by a simple and one-step condensation reaction (Scheme 1). In the present work, the fluorometric property of a dihydrazone-based Schiff base, derived from the condensation of oxalic acid dihydrazide with 2-hydroxypropiophenone, is reported for the selective detection of Al^{3+} ions in aqueous ethanol. Synthetic ease, low cost, and low detection limit may establish H_2hpohas a promising molecular sensor for the *in vitro* or *in vivo* detection of Al^{3+} ions.

2. Experimental

2.1. Materials and methods

Analytical grade chemicals were obtained from commercial sources. Chloride salts of all metals, 2-hydroxypropiophenone, oxalic acid dihydrazide, and solvents were purchased from Merck Chemicals, India, or SD Fine Chemicals Limited and used as such. Ethanol is distilled in the presence of limestone and is used after thoroughly checking its purity using UV-vis and fluorescence spectral techniques [39].

2.2. Synthesis of H_2hpoh

To prepare H_2hpoh, a 30 mL aqueous solution of oxalic acid dihydrazide (5 mmol, 0.59 g) were mixed with 20 mL of ethanolic solution of 2-hydroxypropiophenone (10 mmol, 1.50 mL) in a 1:2 molar ratio in a round bottom flask (Scheme 1). The reaction mixture was refluxed for 4 h and a cream-colored crystalline product was obtained upon cooling of the above solution at room temperature. The product was filtered using a Buchner funnel and purified by washing several times with water followed by ethanol to remove the unreacted components. The pure compound was dried in a desiccator over anhydrous calcium chloride at room temperature.

N'^{1}, *N*'^{2}-*bis*((*E*)-1-(2-hydroxyphenyl)propylidene)oxalohydrazide (H_2hpoh): Color: Cream. Yield: 75%. M.p.: > 300 °C. FT-IR (KBr, ν, cm^{-1}): ν(O-H),3359 (br); ν(N-H), 3285 (br); ν(C=O), 1658; ν(C=N), 1568; ν(C-OH), 1338; ν(N-N), 967. ^{1}H NMR (300 MHz, DMSO-d_6, δ, ppm): 13.019 (s, 2H, Enolic-OH), 11.990 (s, 2H, Ar-OH), 9.992 (s, 2H, NH), 7.681-6.842 (8H, Ar-H), 4.511 (s, 4H, CH_2), 1.140 (s, 6H, CH_3). ^{13}C NMR (75 MHz, DMSO-d_6, δ, ppm): 164.80 (C=O), 159.69 (C-OH), 158.66 (C=N), 158.35 (C=N), 132.30-118.12 (Aromatic carbons), 20.11 (CH_2), 11.79 (CH_3). MS (ESI, *m/z* (%)): 383.1, (calc: 382.41).

2.3. Instrumentation

The ^{1}H and ^{13}C NMR spectra were recorded on a Bruker Avance IIIHD FT-NMR spectrophotometer (300 MHz). A JEOL AL-300 FT-NMR (300 MHz) multinuclear spectrometer is used for NMR titration, for which tetramethylsilane (TMS) is used as an internal standard. The PerkinElmer FT-IR spectrophotometer is utilized to record the infrared spectrum in the spectral range of 400-4000 cm^{-1} using the KBr Pallet method. A Shimadzu Pharmaspec UV-1700 spectrophotometer is used to record the electronic absorption spectra in a water-ethanol mixture (1:4). Fluorescence spectra were recorded on a Horiba Jobin-Yvon Fluorolog3 spectrofluorometer (Model FL3-11). The Oxford Diffraction Gemini Diffractometer equipped with a graphite monochromated MoKα (λ = 0.71073 Å) radiation source is utilized for the collection of single-crystal X-ray diffraction data of H_2hpoh at 293(2) K. The structure was solved by the direct method (SHELXL-97) and full-matrix least-squares on F^2 using anisotropic displacement parameters for all non-hydrogen atoms is applied for refinement of all data. All hydrogen atoms were included in the refinement at a geometrically ideal position and refined with a riding model [40,41]. The structures of H_2hpoh were generated using Mercury and ORTEP-3 software packages [42,43].

3. Results and discussion

As is well known about the existence of amide/hydrazide in *keto*-amine and *enol*-imine tautomeric structures, the prepared probe may exist in the following tautomeric structures (Scheme 2). From the chemical structure, it is clear that the *enol*-imine form is highly conjugated compared to the *keto*-amine form. Hence, in the *keto*-amine form, various rotational states are possible for non-radiative decay during electronic transitions, whereas such states are not possible in the *enol*-imine form. The solution of H_2hpoh is weakly fluorescent, suggesting a dynamic tautomerism with a major contribution of *keto*-amine form. The change in fluorescence properties upon reaction with metals may be due to the interaction of metal ions with H_2hpoh in the particular tautomeric form which is discussed later.

In the FT-IR spectrum of the H_2hpoh receptor, the characteristic stretching vibrations of OH and NH, C=O, C=N, and C-O appear at 3359, 3285,1658, 1568 and 1338 cm^{-1}, respectively [25-28]. Characteristic signals of Ar-OH and NH protons in the ^{1}H NMR of H_2hpoh appear at δ 11.990 and 9.992 ppm, respectively. The additional signal appears at δ 13.019 ppm for the enolic OH proton due to the *keto-enol* tautomeric resonance. Whereas, aromatic protons resonate between δ 7.681-6.842 ppm and the aliphatic CH_2 and CH_3 protons of propiophenone resonates at δ 4.511 and 1.140 ppm, respectively. The peaks appear with shoulder not multiplets in the aromatic and aliphatic region due to dynamic *keto-enol* tautomeric resonance.

Table 1. Crystal data and structure refinement for H_2hpoh.

Empirical formula	$C_{20}H_{22}N_4O_4$
Formula weight (g/mol)	382.41
Temperature (K)	293(2)
Crystal system	Monoclinic
Space group	$P2_1/c$
a, (Å)	6.0747(15)
b, (Å)	11.621(5)
c, (Å)	13.453(4)
α (°)	90
β (°)	94.61(3)
γ (°)	90
Volume (Å^3)	946.6(5)
Z	2
ρ_{calc}(g/cm^3)	1.342
μ (mm^{-1})	0.096
F(000)	404.0
Crystal size (mm^3)	0.24 × 0.22 × 0.19
Radiation	MoKα (λ = 0.71073)
2Θ range for data collection (°)	6.076 to 58.05
Index ranges	$-8 \le h \le 5$, $-15 \le k \le 15$, $-16 \le l \le 12$
Reflections collected	4046
Independent reflections	2149 [R_{int} = 0.0876, R_{sigma} = 0.2223]
Data/restraints/parameters	2149/0/131
Goodness-of-fit on F^2	0.997
Final R indexes [I≥2σ (I)]	R_1 = 0.0972, wR_2 = 0.1488
Final R indexes [all data]	R_1 = 0.2993, wR_2 = 0.2316
Largest diff. peak/hole (e.Å^{-3})	0.23/-0.23

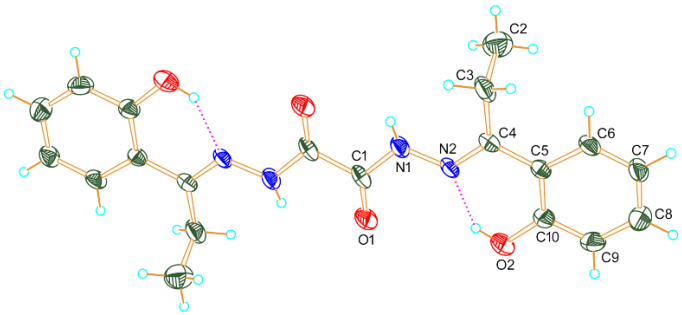

Figure 1. ORTEP diagram of H_2hpoh with atom labeling. The dotted bonds are intramolecular H-bonding.

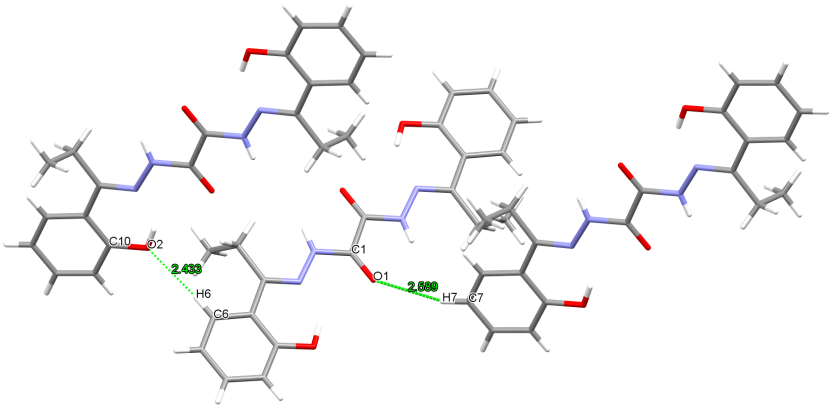

Figure 2. Intermolecular C-H···O interaction between H_2hpoh molecules.

Similarly, characteristic peaks of >*C*=O, *C*–OH, >*C*=N–, >*C*H$_2$ and –*C*H$_3$ in the ^{13}C NMR spectrum of H_2hpoh appear at δ 164.80, 159.69, 158.66 & 158.35, 20.11 and 11.79 ppm, respectively, and aromatic carbons resonate between δ 132.30-118.12 ppm. In the electrospray ionization mass spectra (ESI-MS) of H_2hpoh, the peak of the molecular ion observed at *m/z* = 383.1 corresponds to [M+H]$^+$.

Finally, the structural characterization of H_2hpoh was performed using a single crystal XRD study and the ORTEP diagram with atom labeling scheme is presented in Figure 1. This probe crystallizes in the monoclinic $P2_1/c$ space group (Table 1). The bond distance O(1)-C(1) (1.208 Å) and N(2)-C(4) (1.297 Å) corresponds to the double bond character of the >C=O and >C=N– bond (Table 2). It suggests that H_2hpoh exists as a *keto*-amine form in the solid state.

The presence of an intramolecular hydrogen bond O(2)-H(2)···N(2) between O(2)-H(2) of the phenyl ring and the imine-N atom in the crystal structure of H_2hpoh indicates the stabilization of the *keto*-amine form (Table 3) [25,28]. Along with intramolecular hydrogen bonds, intermolecular C-H···O led to a one-dimensional chain (Figure 2) and the intermolecular C···C interaction between phenolic and carboxylic carbons of adjacent molecules led to a stacked structure (Figure 3).

Table 2. Bond length, bond angle, and torsion angle for H_2hpoh.

Atom	Atom			Length (Å)	Atom	Atom			Length (Å)
O1	C1			1.208(6)	C6	C7			1.367(6)
O2	C10			1.346(6)	C7	C8			1.362(7)
N2	N1			1.370(6)	C3	C4			1.527(7)
N2	C4			1.297(6)	C3	C2			1.487(7)
N1	C1			1.343(6)	C10	C9			1.391(6)
C5	C6			1.410(6)	C9	C8			1.381(7)
C5	C10			1.392(7)	C1	C1[1]			1.528(10)
C5	C4			1.463(6)					
Atom	**Atom**	**Atom**		**Angle (°)**	**Atom**	**Atom**	**Atom**		**Angle (°)**
C4	N2	N1		119.9(5)	C9	C10	C5		119.4(5)
C1	N1	N2		117.0(5)	N2	C4	C5		114.6(5)
C6	C5	C4		121.2(5)	N2	C4	C3		124.7(5)
C10	C5	C6		117.4(5)	C5	C4	C3		120.7(5)
C10	C5	C4		121.4(5)	C8	C9	C10		121.7(6)
C7	C6	C5		122.0(5)	O1	C1	N1		126.3(5)
C8	C7	C6		120.2(6)	O1	C1	C1[1]		122.5(6)
C2	C3	C4		110.1(5)	N1	C1	C1[1]		111.2(6)
O2	C10	C5		124.4(5)	C7	C8	C9		119.2(6)
O2	C10	C9		116.2(5)					
A	**B**	**C**	**D**	**Angle (°)**	**A**	**B**	**C**	**D**	**Angle (°)**
O2	C10	C9	C8	-179.9(5)	C6	C7	C8	C9	-0.6(9)
N2	N1	C1	O1	-3.1(9)	C10	C5	C6	C7	-0.9(8)
N2	N1	C1	C1[1]	178.8(5)	C10	C5	C4	N2	-1.7(7)
N1	N2	C4	C5	-179.9(4)	C10	C5	C4	C3	175.1(5)
N1	N2	C4	C3	3.3(8)	C10	C9	C8	C7	1.0(10)
C5	C6	C7	C8	0.6(8)	C4	N2	N1	C1	-173.8(5)
C5	C10	C9	C8	-1.4(9)	C4	C5	C6	C7	-180.0(5)
C6	C5	C10	O2	179.7(5)	C4	C5	C10	O2	-1.3(8)
C6	C5	C10	C9	1.3(8)	C4	C5	C10	C9	-179.6(5)
C6	C5	C4	N2	177.3(5)	C2	C3	C4	N2	-98.5(6)
C6	C5	C4	C3	-5.8(8)	C2	C3	C4	C5	85.0(6)

[1] Symmetry code: 2-*x*, -*y*, -*z*.

Table 3. Hydrogen bond parameters (Å and °) in the H_2hpoh.

D–H···A	D–H	H···A	D···A	< (DHA)
O(2)–H(2)···N(2)	0.82	1.79	2.503(6)	144
N(1)–H(1)···O(1)	0.80(5)	2.27(6)	2.673(6)	111(5)
C(3)–H(3B)···N(1)	0.97	2.51	2.849(8)	100
C(6)–H(6)···O(2)	0.93	2.43	3.325(7)	161
C(7)–H(7)···O(1)	0.93	2.59	3.493(7)	164

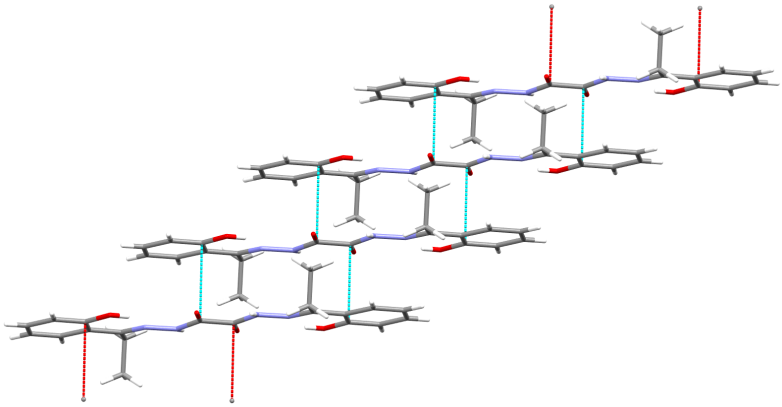

Figure 3. Intermolecular C···C interaction between phenolic and carboxylic carbons.

The sensing properties of H_2hpoh have been investigated by means of UV-visible/fluorescence aqueous ethanol titration (water:ethanol mixture, 1:4) and ^{1}H NMR titration in DMSO-d_6 at room temperature. The absorption spectral band that appears at 335 nm corresponds to a yellow-green solution. A solution of H_2hpoh (50 μM) in aqueous ethanol was used for UV-visible titration experiments and triple distilled water is used to prepare solutions of metal chloride salts. The addition of an aqueous solution of Al^{3+} ions (100 μM) to aqueous ethanolic solutions, each of H_2hpoh (50 μM) led to a shift in the absorption band from 335 to 382 nm (bathochromic shift of ~47 nm) with a decrease in the intensity of absorption. As a result, the color of the solution turned from yellow-green to intense green, which is visible with the naked eye.

Not only have, we performed UV-visible titration of H_2hpoh with direct addition of two equivalents of aqueous Al^{3+} ions (Figure 4a), but we also performed UV-visible titration of H_2hpoh by gradual addition of aqueous Al^{3+} in 0-5 equivalents (Figure 4b). Furthermore, to check the interaction of other metals with H_2hpoh, UV-vis spectra of H_2hpoh with the addition of other metal ions *viz*. Na^+, K^+, Ca^{2+}, Ba^{2+}, Mn^{2+}, Fe^{3+}, Co^{2+}, Ni^{2+}, Cu^{2+}, Zn^{2+}, Cr^{3+}, Cd^{2+} and Hg^{2+} (as chloride) are also performed. Among all metal ions, alkali/alkaline earth metal ions and Mn^{2+} do not produce a significant change in the UV-vis spectra of H_2hpoh, suggesting that only electrostatic interactions are present between metal ions and H_2hpoh. On the other hand, spectral changes are observed in the case of different transition metal ions, which is an indication of metal ions-H_2hpoh binding.

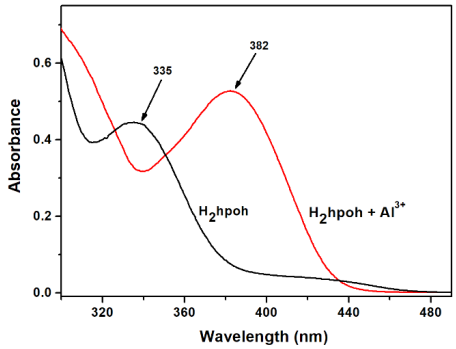

(a)

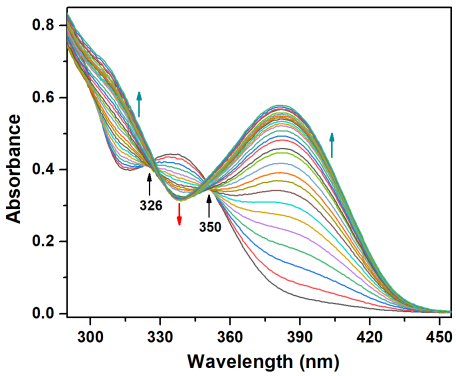

(b)

Figure 4. UV-visible spectra of the H_2hpoh (50 μM) water-ethanol mixture (1:4) without and with the addition of Al^{3+} ions (a) direct addition of 2 equivalents of aqueous Al^{3+} ions, and (b) gradual addition of aqueous Al^{3+} ions (0-5 equivalents).

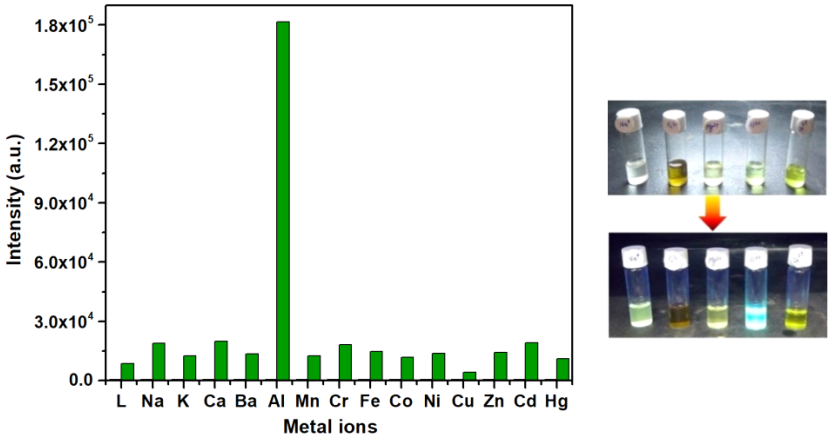

Figure 5. Fluorescence spectra of H_2hpoh (5 μM) + metal ions (100 μM) at λ_{em}: 478 nm (λ_{ex}: 382 nm) in the water-ethanol mixture (1:4), where L = H_2hpoh, M^{n+} = Na^+, K^+, Ca^{2+}, Ba^{2+}, Al^{3+}, Mn^{2+}, Fe^{3+}, Co^{2+}, Ni^{2+}, Cu^{2+}, Zn^{2+}, Cr^{3+}, Cd^{2+} and Hg^{2+}. Inset (Solution of H_2hpoh in the presence of Na^+, Fe^{3+}, Mg^{2+}, Al^{3+}, and Cu^{2+} in visible and UV light).

To determine the binding stoichiometry of H_2hpoh and Al^{3+} ions, electronic absorption spectra are recorded for solutions of H_2hpoh and Al^{3+} ions mixed in varying mole fractions. Finally, from Job's plot, it is clear that the complex formation of Al^{3+} with receptor H_2hpoh is 2:1 stoichiometry, respectively [44].

From the UV-vis study, it is clear that the selectivity for sensing to any metal ion under investigation is not possible employing electronic absorption spectroscopy. Hence, to obtain the selective response of receptor H_2hpoh among metal ions, *i.e.,* Al^{3+}, Na^+, K^+, Ca^{2+}, Ba^{2+}, Mn^{2+}, Fe^{3+}, Co^{2+}, Ni^{2+}, Cu^{2+}, Zn^{2+}, Cr^{3+}, Cd^{2+} and Hg^{2+}, electronic emission studies were also performed (Figure 5). The solution of the pure receptor H_2hpoh shows weak fluorescence at λ_{em} = 478 nm when excited at λ_{ex} = 382 nm, no significant change in the fluorescence intensity is observed upon the addition of other metals. However, the solution of H_2hpoh with two equivalent aqueous solutions of Al^{3+} ions exhibit very high intensity fluorescence spectra (Figure 6). This distinct change in color from light yellow-green to intense green is visible under UV light, suggesting the formation of a strong fluorescent complex of H_2hpoh with Al^{3+}.The gradual addition of Al^{3+} to H_2hpoh in fluorescence titration also supports the fluorescence *turn-on* of H_2hpoh by Al^{3+} (Figure 6b).

Among the various possibilities for quenching fluorescence in pure H_2hpoh, *cis-trans* isomerization across the >C=N- bond and intramolecular charge transfer (ICT) in hydrazone-based receptors are the most probable [45]. Fluorescence enhancement upon addition of Al^{3+} ions to H_2hpoh may be due to inhibition of *cis-trans* isomerization [46] and/or reduction in the ICT effect due to the chelation of H_2hpoh with Al^{3+}.

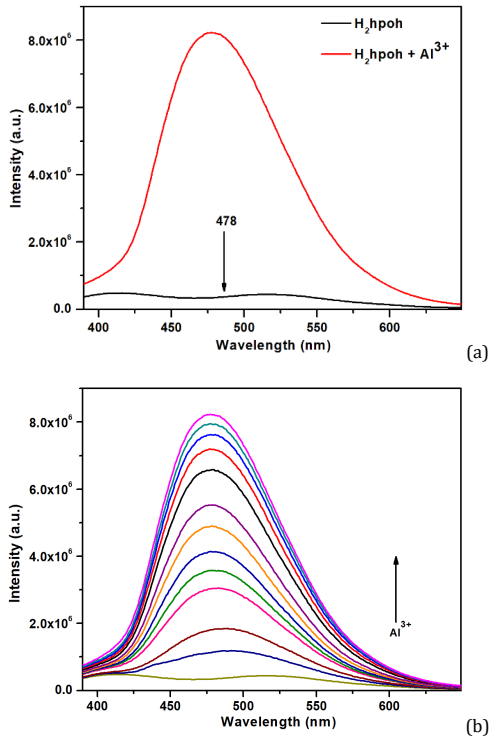

Figure 6. Fluorescence of H_2hpoh (50 μM) in a water-ethanol mixture (1:4) without and with the addition of Al^{3+} ions (a) direct addition of two equivalents of aqueous Al^{3+} ions, and (b) gradual addition of aqueous Al^{3+} ions (0-2 equivalents) (λ_{em}: 478 nm, λ_{ex}: 382 nm).

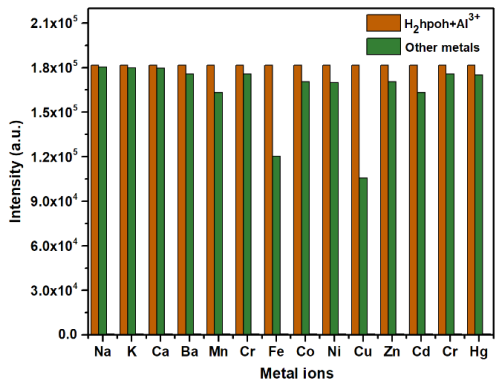

Figure 7. Interference study in a binary solution of H_2hpoh (5 μM) + Al^{3+} (100 μM) with other metal ions M^{n+} (100 μM), (λ_{em}: 478 nm, λ_{ex}: 382 nm) (where M^{n+} = Al^{3+}, Na^+, K^+, Ca^{2+}, Ba^{2+}, Mn^{2+}, Fe^{3+}, Co^{2+}, Ni^{2+}, Cu^{2+}, Zn^{2+}, Cr^{3+}, Cd^{2+} and Hg^{2+}).

Chelation of Al^{3+} ions with H_2hpoh not only reduces the ICT effect, but also restricts the free rotation around the carbon of azomethine attached to the aromatic ring. As a result of rotation restriction, nonradiative decay processes are hindered, resulting in a significant enhancement of the fluorescence intensity. Such enhancement in fluorescence intensity upon chelation of metal ions with the receptor is known as chelation enhanced fluorescence (CHEF) [47-49].

Most of the metal ions do not show interference in the detection of Al^{3+} by H_2hpoh except Fe^{3+} and Cu^{2+} in aqueous ethanol. Although the direct addition of Fe^{3+} and Cu^{2+} to the solution of H_2hpoh does not cause a significant change in the fluorescence spectra, the addition of these ions to the binary solution of H_2hpoh (5 μM) + Al^{3+} (100 μM) results inhibition of the fluorescence intensity (Figure 7). The smaller ionic radii (0.5 Å) of the Al^{3+} ion may be responsible for the selectivity of H_2hpoh towards Al^{3+} by along with appropriate coordination geometry for the chelating receptor H_2hpoh and the higher charge density (R = 4.81) of the Al^{3+} ion may be responsible for the strong coordination ability of Al^{3+} with H_2hpoh [49].

Fluorescence responses are very fast after the addition of Al^{3+} to H_2hpoh and the maximum fluorescence has been observed after the addition of two equivalents of aqueous Al^{3+}in a 5 μM aqueous ethanolic solution of H_2hpoh. Consequently, the binding constant (K_B) is obtained from the linear fitting of the fluorescence titration intensities at various concentrations of Al^{3+} ions in the modified Benesi-Hildebrand equations for the stoichiometry of the complex 2:1 (M: L) (Equation (1)) [50].

$$\frac{Io}{I-Io} = \left(\frac{a}{b-a}\right)^2 \left(\frac{1}{K_B[\text{substrate}]^2} + 1\right) \quad (1)$$

where I_o and I are the fluorescence intensity of H_2hpoh at 478 nm in the absence and in the presence of various concentrations of Al^{3+}; a, b are constants; [substrate] is the concentration of Al^{3+}.

Table 4. Comparison of binding constant and detection limit.

Compound	M:L	Binding constant K_b (M^{-1})	Detection limit (M)	References
N,N'-bis((2-hydroxynaphthalen-1-yl)methylene)oxa-lohydrazide(H_2ohn) with Al^{3+}	2:1	2.62×10^{11}	8.56×10^{-10}	[25]
o-Hydroxypropiophenone-2-thiophenoyl hydrazone,tcph with Al^{3+}	1:1	5.00×10^{6}	1.35×10^{-9}	[27]
N,N'-bis((2-Hydroxynaphthalen-1-yl)methylene)malo-nohydrazide (H_2nmh) with Al^{3+}	2:1	5.74×10^{9}	5.78×10^{-8}	[28]
(*E*)-2-(2-Aminothiazol-5-yl)-*N'*-((2-hydroxynaphthalen-1-yl)methylene)acetohydrazide (NTH) with Al^{3+}	1:1	3.65×10^{9}	1.09×10^{-9}	[36]
β-Pinene-based fluorescent probe (6,6-dimethyl-3-(pyridin-2-yl)-4,5,6,7-tetrahydro-2*H*-5,7-methanoindazole)	1:1	1.89×10^{3}	8.10×10^{-8}	[37]
2-((*E*)-1-(2-(Dimethylamino) ethylimino)ethyl)phenol (HL) with Al^{3+}	2:1	2.10×10^{4}	4.32×10^{-6}	[38]
N'^{1},*N'*^{2}-bis{1-(2-Hydroxyphenyl) propylidene}oxalohydrazide(H_2hpoh) with Al^{3+}	2:1	8.99×10^{10}	7.80×10^{-5}	This work

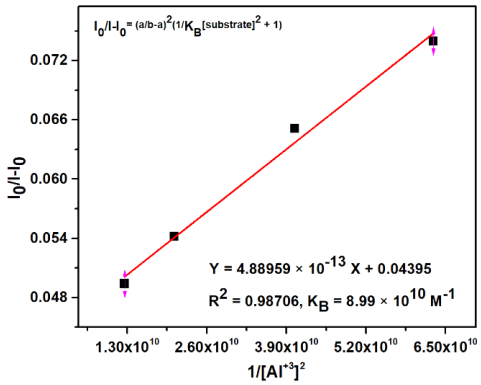

Figure 8. Benesi-Hildebrand plot for H_2hpoh with Al^{3+}, considering the 2:1 complexation. The goodness of fit is shown by the R^2 value.

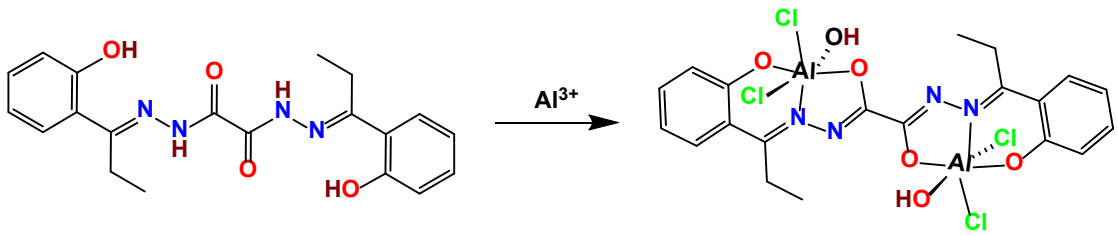

Scheme 3. Proposed reaction between theH_2hpoh and Al^{3+} ions.

Observation of the linear fit in $I_o/I-I_o$ *vs* $1/[Al^{3+}]^2$ graph and the close agreement of the experimental value of $K_B = 8.99\times10^{10}$ M^{-1} to the theoretical fit, support 2:1 (M:L) complex stoichiometry (Figure 8). The high binding constant is consistent with the highly selective sensing of Al^{3+} with H_2hpoh without the interference of most metal ions. The detection limit (LOD) of H_2hpoh can be calculated based on Equation (2) [51].

$$\text{Detection limit} = \frac{3\sigma}{\text{slope}} \quad (2)$$

where standard deviation (σ is calculated by recording the fluorescence intensity of H_2hpoh without Al^{3+} by 10 times. A plot of fluorescence intensity as a function of the concentration of the added metal ion provides the value of slope. The detection limit was found to be 7.8×10^{-5} M in the linearity range of 4.99×10^{-7}-7.99×10^{-6} M (R^2 = 0.99824). A comparative table of detection limit and binding constants for some receptors of Al^{3+} with different binding ratios is provided in Table 4. From Table 4, it is clear that although the binding constant of H_2hpoh with Al^{3+} is very high, the detection limit is in order of μM only.

The interaction of the H_2hpoh receptor with Al^{3+} is also supported by the NMR study (Figure 9). ^{1}H NMR titrations have been performed by concomitant addition of Al^{3+} (1×10^{-1} M solution in D_2O) to a 1×10^{-3} M solution of receptors in DMSO-d_6. Upon addition of Al^{3+}, the peak corresponding to the amine proton disappears and the phenolic OH proton shifts slightly downfield with the reduction in peak intensity, suggesting the enolization of the >C=O group and the interaction of Al^{3+} with phenolic OH. The general changes in ^{1}H NMR spectra indicate the complexation between Al^{3+} and H_2hpoh in the deprotonated *enol*-imine form through carbonylate-O, azomethine-N, and phenolic-OH. On the basis of spectroscopic characterization, the proposed structure of H_2hpoh-Al^{3+} complex might be according to Scheme 3. The proposed structure is supported further by theoretical studies.

Density functional theoretical (DFT) calculations have been employed for structural optimization and TD-DFT calculations of H_2hpoh and its Al(III) complex using the *C*1 point group. For both H_2hpoh and its Al(III) complex, Becke's three-parameterized Lee-Yang-Parr (B3LYP) exchange functional with basis sets 6-31G* for all C, H, N, O, and Al atoms has been used in the Gaussian-03 program [52].The geometry around each Al^{3+} is considered a distorted octahedral in which three coordination sites are occupied by one carbonylate-O, one azomethine-N, and one phenolic OH of H_2hpoh,and the other three coordination sites are occupied by two chloride ions and one water molecule. The energy (RB+HF-LYP) was found to be -1295.6107 a.u. and -3773.4669 a.u., respectively, for H_2hpoh and its Al^{3+} complex. The energy level of HOMO and LUMO as well as the bandgap of H_2hpoh is much higher than its Al^{3+} complex; therefore, the thermodynamically favorable conversion of H_2hpoh to H_2hpoh-Al^{3+} (Figure 10) with a bathochromic shift in the UV-visible spectra of the H_2hpoh-Al^{3+} complex. Based on Job's plot, NMR titrations, and DFT calculation, it can be predicted that each molecule H_2hpoh interacts with two Al^{3+} ions in a dibasic hexadentate mode to form the $[Al_2Cl_4(hpoh)(H_2O)_2]$ complex.

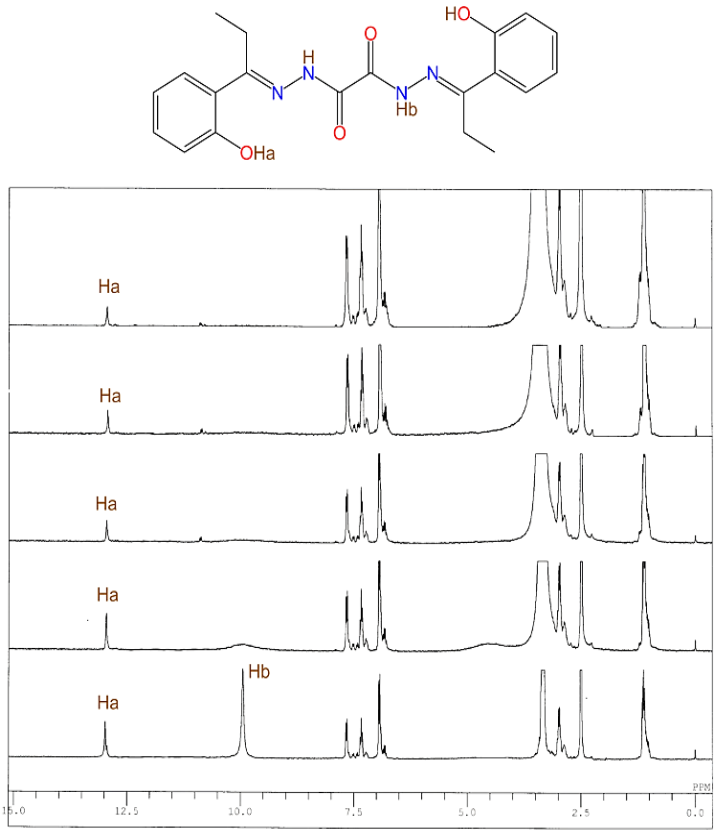

Figure 9. ^{1}H NMR titration of H_2hpoh upon adding 0-2 equivalents of Al^{3+} in DMSO-d_6.

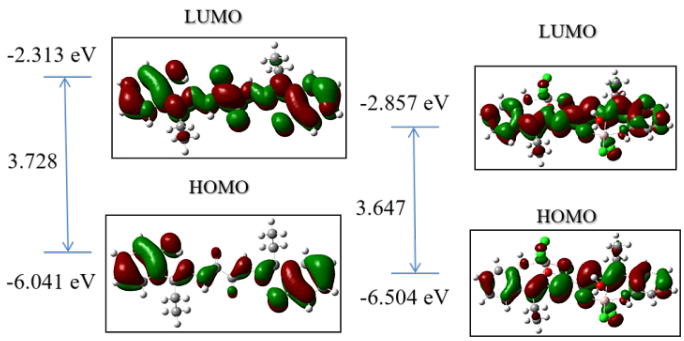

Figure 10. Diagram of the energy level for the frontier π molecular orbitals of H_2hpoh (left) and its Al^{3+} complex (right).

4. Conclusions

In this study, we are exploring the possibility of the preparation of a highly efficient fluorescent probe H_2hpoh for selective detection of the Al^{3+} ion. The synthetic ease, low-cost, and high efficiency of dihydrazone-based fluorescent probes may be a milestone towards the development of a fluorescence-based chemical sensor for metal ions in biological systems. Fluorescence *turn-on* is due to the reduction in the ICT and the restricted rotation of the >C=N- bond in H_2hpoh or chelation-enhanced fluorescence after the binding of Al^{3+} ions. From UV-vis, fluorescence and ^{1}H NMR titration experiments, the stoichiometry of the H_2hpoh-Al^{3+} complex was established to be 2:1 (M:L). The binding of hexadentate H_2hpoh with each $Al^{3+}$is carried out through one carbonylate-O, one azomethine-N, and phenolic OH and the remaining coordination site of $Al^{3+}$is completed by chloride and water ligands. From the fluorescence study, the binding constant (K_B) and detection limit for Al^{3+} were also determined. The structure of H_2hpoh is established by a single crystal X-ray diffraction study, while the structure of the H_2hpoh-Al^{3+} complex is established by DFT calculations.

Acknowledgments

The authors thank the Head of the Sophisticated Analytical Instrument Facility for NMR, Single-crystal XRD Institute of Science, Banaras Hindu University; Central Drug Research Institute, Lucknow, India for extending the ESI-MS facility. Ashish Kumar Singh acknowledges the Department of Science and Technology for the INSPIRE Faculty Fellowship (Award Number: DST/INSPIRE/04/2015/002001).

Supporting information S

CCDC-985204 contains the supplementary crystallographic data for this paper. These data can be obtained free of charge via www.ccdc.cam.ac.uk/data_request/cif, or by e-mailing data_request@ccdc.cam.ac.uk, or by contacting The Cambridge Crystallographic Data Centre, 12 Union Road, Cambridge CB2 1EZ, UK; fax: +44(0)1223-336033.

Disclosure statement

Conflict of interest: There are no conflicts to declare.
Ethical approval: All ethical guidelines have been adhered.
Sample availability: Samples of the compound are available from the author.

CRediT authorship contribution statement

Conceptualization: Chandani Singh, Romi Dwivedi; Methodology: Chandani Singh, Divya Pratap Singh, Ashish Kumar Singh; Software: Divya Pratap Singh, Ashish Kumar Singh; Validation: Divya Pratap Singh, Ashish Kumar Singh; Formal Analysis: Chandani Singh, Romi Dwivedi; Investigation: Chandani Singh, Divya Pratap Singh, Ashish Kumar Singh; Resources: Sunil Kumar Singh, Vinod Prasad Singh; Data Curation: Sunil Kumar Singh, Vinod Prasad Singh; Writing - Original Draft: Divya Pratap Singh, Sunil Kumar Singh, Ashish Kumar Singh; Writing - Review and Editing: Divya Pratap Singh, Sunil Kumar Singh, Ashish Kumar Singh, Vinod Prasad Singh; Visualization: Sunil Kumar Singh, Vinod Prasad Singh; Funding acquisition: Ashish Kumar Singh, Vinod Prasad Singh; Supervision: Sunil Kumar Singh, Divya Pratap Singh, Ashish Kumar Singh; Project Administration: Divya Pratap Singh, Ashish Kumar Singh.

Funding

Department of Science and Technology for INSPIRE Faculty Fellowship (Award Number: DST/INSPIRE/04/2015/002001).

ORCID and Email

Chandni Singh
chandani0905@gmail.com
https://orcid.org/0000-0002-9052-403X
Divya Pratap Singh
dpsingh_011@yahoo.co.in
dpsbhu11@gmail.com
dpsingh@gecazamgarh.ac.in
https://orcid.org/0000-0001-8760-4031
Sunil Kumar Singh
singh.skumar@gmail.com
https://orcid.org/0000-0003-2095-6723
Romi Dwivedi
dwivediromi26@gmail.com
https://orcid.org/0000-0002-0485-4156
Ashish Kumar Singh
ashish.bhuchem@gmail.com
https://orcid.org/0000-0001-9499-5843
Vinod Prasad Singh
singvp@yahoo.co.in
https://orcid.org/0000-0002-2997-5333

References

[1]. Roy, P. Recent advances in the development of fluorescent chemosensors for Al3. *Dalton Trans.* **2021**, *50*, 7156–7165.
[2]. Gupta, A.; Kumar, N. A review of mechanisms for fluorescent "'turn-on"' probes to detect Al3+ ions. *RSC Adv.* **2016**, *6*, 106413–106434.
[3]. Li, B.; He, T.; Fan, Y.; Yuan, X.; Qiu, H.; Yin, S. Recent developments in the construction of metallacycle/metallacage-cored supramolecular polymers via hierarchical self-assembly. *Chem. Commun. (Camb.)* **2019**, *55*, 8036–8059.
[4]. He, L.; Dong, B.; Liu, Y.; Lin, W. Fluorescent chemosensors manipulated by dual/triple interplaying sensing mechanisms. *Chem. Soc. Rev.* **2016**, *45*, 6449–6461.
[5]. Das, S.; Dutta, M.; Das, D. Fluorescent probes for selective determination of trace level Al3+: recent developments and future prospects. *Anal. Methods* **2013**, *5*, 6262–6285.
[6]. Hwang, I. H.; Choi, Y. W.; Kim, K. B.; Park, G. J.; Lee, J. J.; Nguyen, L.; Noh, I.; Kim, C. A highly selective and sensitive fluorescent turn-on Al3+ chemosensor in aqueous media and living cells: experimental and theoretical studies. *New J Chem* **2016**, *40*, 171–178.
[7]. Alici, O.; Aydin, D. A Schiff-base receptor based on phenolphthalein derivate appended 2-furoic hydrazide: Highly sensitive fluorogenic "turn on" chemosensor for Al3+. *J. Photochem. Photobiol. A Chem.* **2021**, *404*, 112876.
[8]. Na, N.; Wang, F.; Huang, J.; Niu, C.; Yang, C.; Shang, Z.; Han, F.; Ouyang, J. An aggregation-induced emission-based fluorescent chemosensor of aluminium ions. *RSC Adv.* **2014**, *4*, 35459–35462.
[9]. Maity, D.; Govindaraju, T. A differentially selective sensor with fluorescence turn-on response to Zn2+ and dual-mode ratiometric response to Al3+ in aqueous media. *Chem. Commun. (Camb.)* **2012**, *48*, 1039–1041.
[10]. Sahana, S.; Bose, S.; Mukhopadhyay, S. K.; Bharadwaj, P. K. A highly selective and sensitive turn-on fluorescence chemosensor based on a rhodamine–adenine conjugate for Al 3+ in aqueous medium: Bio-imaging and DFT studies. *J. Lumin.* **2016**, *169*, 334–341.
[11]. Ghanbari, B.; Zarepour-jevinani, M. Promotional effect of macro cyclization in O2Nx naphtha-aza-crown macrocyclic ligands on fluorescence chemosensing of Al(III). *J. Lumin.* **2019**, *205*, 219–227.
[12]. Wang, M.; Lu, L.; Song, W.; Wang, X.; Sun, T.; Zhu, J.; Wang, J. AIE-active Schiff base compounds as fluorescent probe for the highly sensitive and selective detection of Al3+ ions. *J. Lumin.* **2021**, *233*, 117911.
[13]. Maity, D.; Dey, S.; Roy, P. A two-pocket Schiff-base molecule as a chemosensor for Al3+. *New J Chem* **2017**, *41*, 10677–10685.
[14]. Feng, S.; Pei, F.; Wu, Y.; Lv, J.; Hao, Q.; Yang, T.; Tong, Z.; Lei, W. A ratiometric fluorescent sensor based on g-CNQDs@Zn-MOF for the sensitive detection of riboflavin via FRET. *Spectrochim. Acta A Mol. Biomol. Spectrosc.* **2021**, *246*, 119004.
[15]. Lv, J.; Feng, S.; Ding, Y.; Chen, C.; Zhang, Y.; Lei, W.; Hao, Q.; Chen, S.-M. A high-performance fluorescent probe for dopamine detection based on g-C3N4 nanofibers. *Spectrochim. Acta A Mol. Biomol. Spectrosc.* **2019**, *212*, 300–307.
[16]. Peng, H.-N.; Liu, Y.-Q.; Huang, J.-Q.; Huang, S.-S.; Cai, X.-P.; Xu, S.-J.; Huang, A.; Zeng, Q.; Xu, M. A simple fluorescent probe for selective detection of Al3+ based on furan Schiff base and its crystal structure. *J. Mol. Struct.* **2021**, *1229*, 129866.
[17]. Kumar, M.; Kumar, A.; Kishor, S.; Kumar, S.; Kumar, A.; Manav, N.; Bhagi, A. K.; Kumar, S.; John, R. P. N-diethylaminosalicylidene based "turn-on" fluorescent Schiff base chemosensor for Al3+ ion: Synthesis, characterisation and DFT/TD-DFT studies. *J. Mol. Struct.* **2022**, *1247*, 131257.
[18]. Upadhyay, K. K.; Kumar, A. Pyrimidine based highly sensitive fluorescent receptor for Al3+ showing dual signalling mechanism. *Org. Biomol. Chem.* **2010**, *8*, 4892–4897.
[19]. Salarvand, Z.; Amirnasr, M.; Meghdadi, S. Colorimetric and fluorescent sensing of Al3+ by a new 2-hydroxynaphthalen based Schiff base "Off-On" chemosensor. *J. Lumin.* **2019**, *207*, 78–84.
[20]. Roy, A.; Dey, S.; Halder, S.; Roy, P. Development of a new chemosensor for Al3+ ion: Tuning of properties. *J. Lumin.* **2017**, *192*, 504–512.
[21]. Tang, X.; Wang, Y.; Han, J.; Ni, L.; Zhang, H.; Li, C.; Li, J.; Qiu, Y. A novel fluorescent probe based on biphenyl and rhodamine for multi-metal ion recognition and its application. *Dalton Trans.* **2018**, *47*, 3378–3387.
[22]. Wang, Q.; Sun, H.; Jin, L.; Wang, W.; Zhang, Z.; Chen, Y. A novel turn on and reversible sensor for Al3+ and its applications in bioimaging. *J. Lumin.* **2018**, *203*, 113–120.
[23]. Li, Z.; Wang, Q.; Wang, J.; Jing, X.; Wang, S.; Xiao, L.; Li, L. A fluorescent light-up probe for selective detection of Al3+ and its application in living cell imaging. *Inorganica Chim. Acta* **2020**, *500*, 119231.
[24]. Shweta, S.; Neeraj, N.; Asthana, S. K.; Mishra, R. K.; Upadhyay, K. K. Design-specific mechanistic regulation of the sensing phenomena of two Schiff bases towards Al3+. *RSC Adv.* **2016**, *6*, 55430–55437.
[25]. Pratap Singh, D.; Singh, V. P. A dihydrazone based fluorescent probe for selective determination of Al3+ ions. *J. Lumin.* **2014**, *155*, 7–14.
[26]. Singh, V. P.; Tiwari, K.; Mishra, M.; Srivastava, N.; Saha, S. 5-[(2-Hydroxynaphthalen-1-yl)methyleneamino]pyrmidine-2,4(1H,3H)-dione as Al3+ selective colorimetric and fluorescent chemosensor. *Sens. Actuators B Chem.* **2013**, *182*, 546–554.
[27]. Dwivedi, R.; Singh, D. P.; Chauhan, B. S.; Srikrishna, S.; Panday, A. K.; Choudhury, L. H.; Singh, V. P. Intracellular application and logic gate behavior of a 'turn off-on-off' type probe for selective detection of Al3+ and F– ions in pure aqueous medium. *Sens. Actuators B Chem.* **2018**, *258*, 881–894.
[28]. Singh, D. P.; Dwivedi, R.; Singh, A. K.; Koch, B.; Singh, P.; Singh, V. P. A dihydrazone based "turn–on" fluorescent probe for selective determination of Al3+ ions in aqueous ethanol. *Sens. Actuators B Chem.* **2017**, *238*, 128–137.
[29]. Alagesan, M.; Bhuvanesh, N. S. P.; Dharmaraj, N. Potentially cytotoxic new copper(II) hydrazone complexes: synthesis, crystal structure and biological properties. *Dalton Trans.* **2013**, *42*, 7210–7223.
[30]. Dwivedi, R.; Singh, D. P.; Singh, S.; Singh, A. K.; Chauhan, B. S.; Srikrishna, S.; Singh, V. P. Logic gate behavior and intracellular application of a fluorescent molecular switch for the detection of Fe3+ and cascade sensing of F- in pure aqueous media. *Org. Biomol. Chem.* **2019**, *17*, 7497–7506.
[31]. Mao, J.; Wang, L.; Dou, W.; Tang, X.; Yan, Y.; Liu, W. Tuning the selectivity of two chemosensors to Fe(III) and Cr(III). *Org. Lett.* **2007**, *9*, 4567–4570.

[32]. Li, Z.; Dai, F.; Wang, J.; Wang, S.; Xiao, L.; Li, L. A selective turn-on fluorescent probe for Al3+ based-on a diacylhydrazone deritive in aqueous medium and its cell imaging. *Synth. Met.* **2020**, *259*, 116234.
[33]. Krishnamoorthy, P.; Sathyadevi, P.; Butorac, R. R.; Cowley, A. H.; Bhuvanesh, N. S. P.; Dharmaraj, N. Variation in the biomolecular interactions of nickel(II) hydrazone complexes upon tuning the hydrazide fragment. *Dalton Trans.* **2012**, *41*, 6842–6854.
[34]. Xing, C.; Hao, L.; Zang, L.; Tang, X.; Zhao, Y.; Lu, J. A highly selective fluorescent probe for Al3+ based on bis(2-hydroxy-1-naphth aldehyde) oxaloyldihydrazone with aggregation-induced emission enhancement and gel properties. *Spectrochim. Acta A Mol. Biomol. Spectrosc.* **2020**, *224*, 117406.
[35]. Liu, Y.; Zhang, L.; Chen, L.; Liu, Z.; Liu, C.; Che, G. 2-Hydroxynaphthalene based acylhydrazone as a turn-on fluorescent chemosensor for Al3+ detection and its real sample applications. *Spectrochim. Acta A Mol. Biomol. Spectrosc.* **2021**, *248*, 119269.
[36]. Gupta, S. R.; Singh, P.; Koch, B.; Singh, V. P. A water soluble, highly sensitive and selective fluorescent probe for Al 3+ ions and its application in live cell imaging. *J. Photochem. Photobiol. A Chem.* **2017**, *348*, 246–254.
[37]. Jiang, Q.; Li, M.; Song, J.; Yang, Y.; Xu, X.; Xu, H.; Wang, S. A highly sensitive and selective fluorescent probe for quantitative detection of Al3+ in food, water, and living cells. *RSC Adv.* **2019**, *9*, 10414–10419.
[38]. Kumar, M.; Kumar, A.; Faizi, M. S. H.; Kumar, S.; Singh, M. K.; Sahu, S. K.; Kishor, S.; John, R. P. A selective 'turn-on' fluorescent chemosensor for detection of Al3+ in aqueous medium: Experimental and theoretical studies. *Sens. Actuators B Chem.* **2018**, *260*, 888–899.
[39]. Perrin, D. D.; Armarego, W. L. F. *Purification of laboratory chemicals*; Pergamon Press: Oxford; New York, 1988.
[40]. Sheldrick, G. M. Phase annealing in SHELX-90: direct methods for larger structures. *Acta Crystallogr. A* **1990**, *46*, 467–473.
[41]. Sheldrick, G. M. SHELXL-97, Program for Crystal Structure Refinement. University of Gottingen, Germany 1997.
[42]. Bruno, I. J.; Cole, J. C.; Edgington, P. R.; Kessler, M.; Macrae, C. F.; McCabe, P.; Pearson, J.; Taylor, R. New software for searching the Cambridge Structural Database and visualizing crystal structures. *Acta Crystallogr. B* **2002**, *58*, 389–397.
[43]. Farrugia, L. J. ORTEP-3 for Windows - a version of ORTEP-III with a Graphical User Interface (GUI). *J. Appl. Crystallogr.* **1997**, *30*, 565–565.
[44]. Job, P. Formation and Stability of Inorganic Complexes in Solution. *Annales de Chimie* **1928**, *10*, 113–203.
[45]. Wu, J.-S.; Liu, W.-M.; Zhuang, X.-Q.; Wang, F.; Wang, P.-F.; Tao, S.-L.; Zhang, X.-H.; Wu, S.-K.; Lee, S.-T. Fluorescence turn on of coumarin derivatives by metal cations: a new signaling mechanism based on C=N isomerization. *Org. Lett.* **2007**, *9*, 33–36.
[46]. Goswami, S.; Paul, S.; Manna, A. A differentially selective chemosensor for a ratiometric response to Zn2+ and Al3+ in aqueous media with applications for molecular switches. *RSC Adv.* **2013**, *3*, 25079.
[47]. Sahana, A.; Banerjee, A.; Das, S.; Lohar, S.; Karak, D.; Sarkar, B.; Mukhopadhyay, S. K.; Mukherjee, A. K.; Das, D. A naphthalene-based Al3+ selective fluorescent sensor for living cell imaging. *Org. Biomol. Chem.* **2011**, *9*, 5523–5529.
[48]. Arduini, M.; Felluga, F.; Mancin, F.; Rossi, P.; Tecilla, P.; Tonellato, U.; Valentinuzzi, N. Aluminium fluorescence detection with a FRET amplified chemosensor. *Chem. Commun. (Camb.)* **2003**, 1606.
[49]. Sen, S.; Mukherjee, T.; Chattopadhyay, B.; Moirangthem, A.; Basu, A.; Marek, J.; Chattopadhyay, P. A water soluble Al3+ selective colorimetric and fluorescent turn-on chemosensor and its application in living cell imaging. *Analyst* **2012**, *137*, 3975–3981.
[50]. Chow, C.-F.; Lam, M. H. W.; Wong, W.-Y. A heterobimetallic ruthenium(II)-copper(II) donor-acceptor complex as a chemo-dosimetric ensemble for selective cyanide detection. *Inorg. Chem.* **2004**, *43*, 8387–8393.
[51]. Long, G. L.; Winefordner, J. D. Limit of detection A closer look at the IUPAC definition. *Anal. Chem.* **1983**, *55*, 712A-724A.
[52]. Frisch, M. J.; Trucks, G. W.; Schlegel, H. B.; Scuseria, G. E.; Robb, M. A.; Cheeseman, J. R.; Montgomery, J. A.; Vreven, T.; Kudin, K. N.; Burant, J. C.; Millam, J. M.; Iyengar, S. S.; Tomasi, J.; Barone, V.; Mennucci, B.; Cossi, M.; Scalmani, G.; Rega, N.; Petersson, G. A.; Nakatsuji, H.; Hada, M.; Ehara, M.; Toyota, K.; Fukuda, R.; Hasegawa, J.; Ishida, M.; Nakajima, T.; Honda, Y.; Kitao, O.; Nakai, H.; Klene, M.; Li, X.; Knox, J. E.; Hratchian, H. P.; Cross, J. B.; Adamo, C.; Jaramillo, J.; Gomperts, R.; Stratmann, R. E.; Yazyev, O.; Austin, A. J.; Cammi, R.; Pomelli, C.; Ochterski, J. W.; Ayala, P. Y.; Morokuma, K.; Voth, G. A.; Salvador, P.; Dannenberg, J. J.; Zakrzewski, V. G.; Dapprich, S.; Daniels, A. D.; Strain, M. C.; Farkas, O.; Malick, D. K.; Rabuck, A. D.; Raghavachari, K; Foresman, J. B.; Ortiz, J. V.; Cui, Q.; Baboul, A. G.; Clifford, S.; Cioslowski, J.; Stefanov, B. B.; Liu, G.; Liashenko, A.; Piskorz, P.; Komaromi, I.; Martin, R. L.; Fox, D. J.; Keith, T.; Al-Laham, M. A.; Peng, C. Y.; Nanayakkara, A.; Challacombe, M.; Gill, P. M. W.; Johnson, B.; Chen, W.; Wong, M. W.; Gonzalez, C.; Pople, J. A. Gaussian, Inc. , Wallingford CT, 2009.